

Figure 1

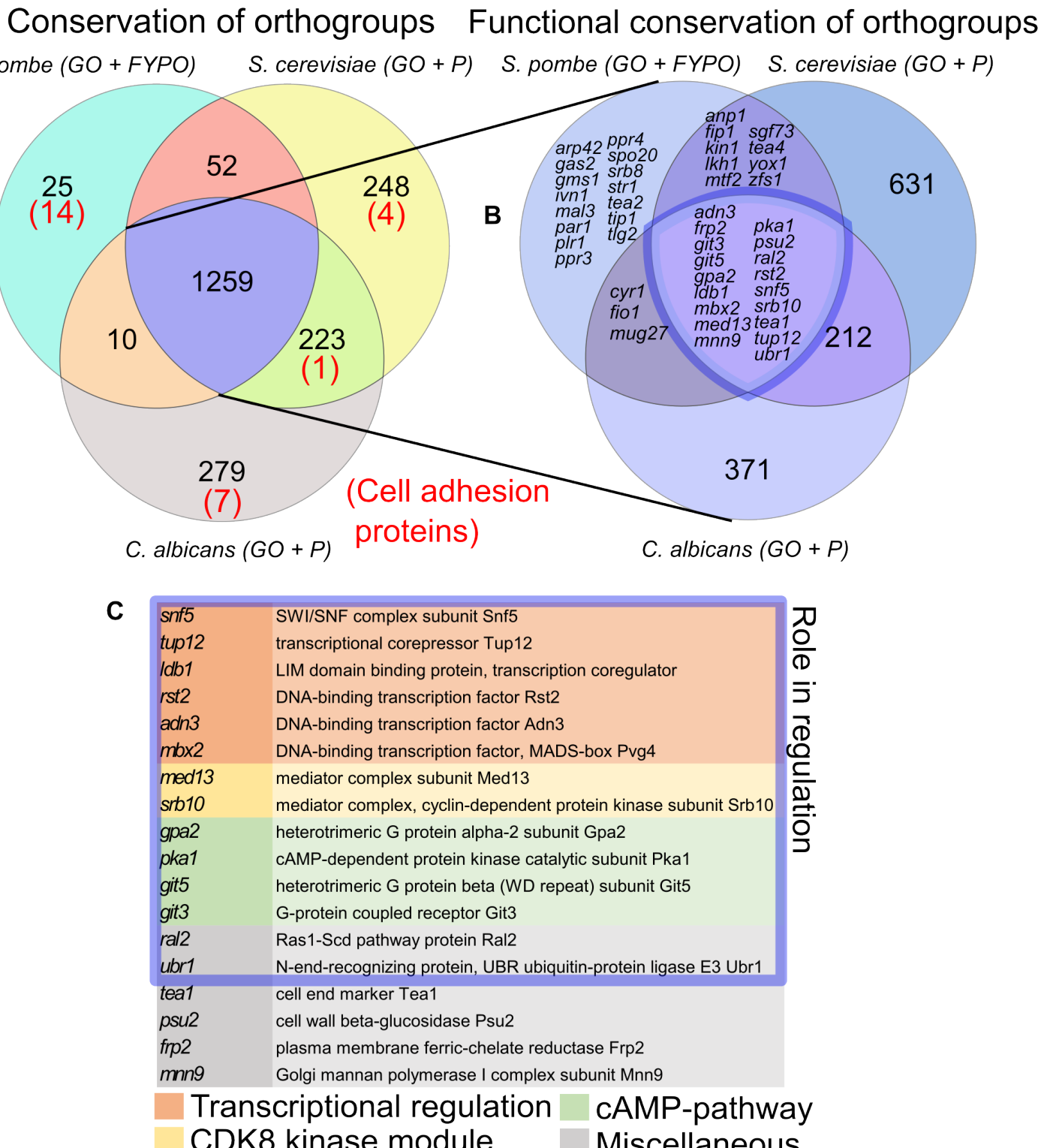


Figure 1: Several regulators of MLP formation are conserved between fission and budding yeast, but cell-adhesion effector proteins are not. A: Venn diagram of orthogroups, in which at least one gene in the orthogroup is annotated in GO-terms or phenotypic data related to MLP formation in either *S. pombe*, *S. cerevisiae* or *C. albicans*. Red numbers indicate cell-adhesion proteins. B: Venn diagram of orthogroups that are conserved across the 3 species (i.e. the middle subset on plot A) asking whether they are also functionally conserved (contain at least one gene that is annotated in GO-terms or phenotypic data related to MLP formation in all three species). C: Table of functionally conserved genes coloured by their broad functional category. GO: Gene Ontology, FYPO: Fission Yeast Phenotype Ontology, P: Phenotype annotations. Venn diagrams were made using matplotlib-venn in Python (120).

Figure 2

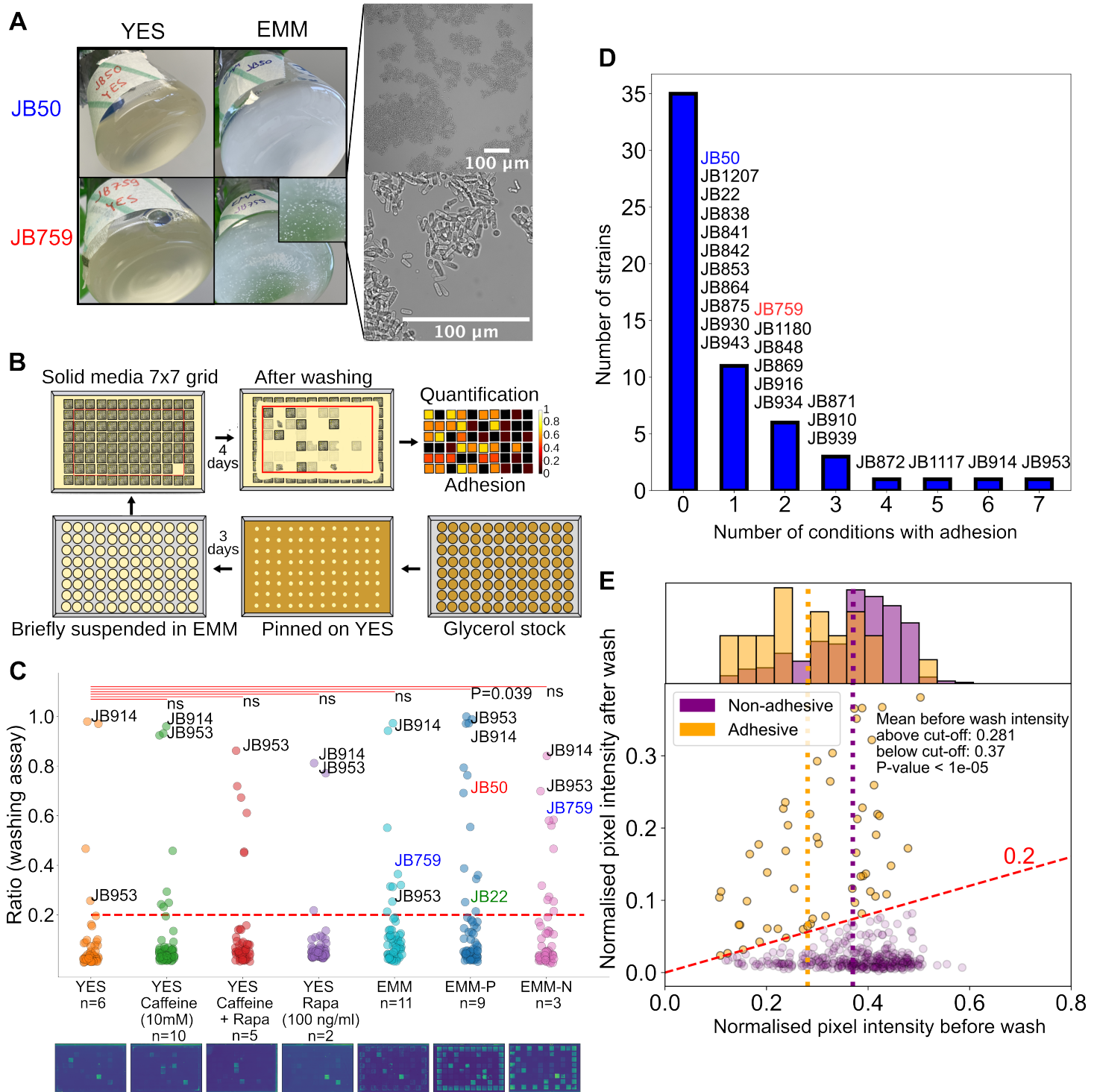


Figure 2: MLP formation in *S. pombe* natural isolates varies with nutrient conditions and is associated with decreased growth. A: Left: Images of our initial observations on the *S. pombe* lab strain JB50 and the natural isolate JB759 showing MLP formation in the JB759 strain in EMM. Right: Microscopy images at two different magnifications of the JB759 strain grown in EMM for 2 days. B: Scheme of the high-throughput adhesion assay used to assess MLP formation in *S. pombe*. C: Strip-plot of adhesion to agar across different conditions in the natural isolate library, with images of representative post-wash agar plates below. Each dot represents the mean adhesion value for a given strain in a specific condition. Dashed line shows a cut-off (intensity after wash greater than 0.2 times before wash intensity) for strong phenotypes. P-values were obtained using a one-sided permutation-based T-test and Bonferroni-correction. Strains around the edges were not taken into account for any statistical analysis (see Methods). D: Histogram showing the number of unique strains forming MLPs in a given number of conditions. E: Scatterplot of mean cell densities before and after washing. Each dot represents one strain in one condition, orange dots represent adhesive data points (ratio of before wash to after wash intensity greater than 0.2, solid red line) and purple dots represent non-adhesive data points. The histogram shows the distribution of cell densities before washing, as a proxy for growth. The dashed orange and purple lines mark the mean pre-wash density for the two populations.

Figure 3

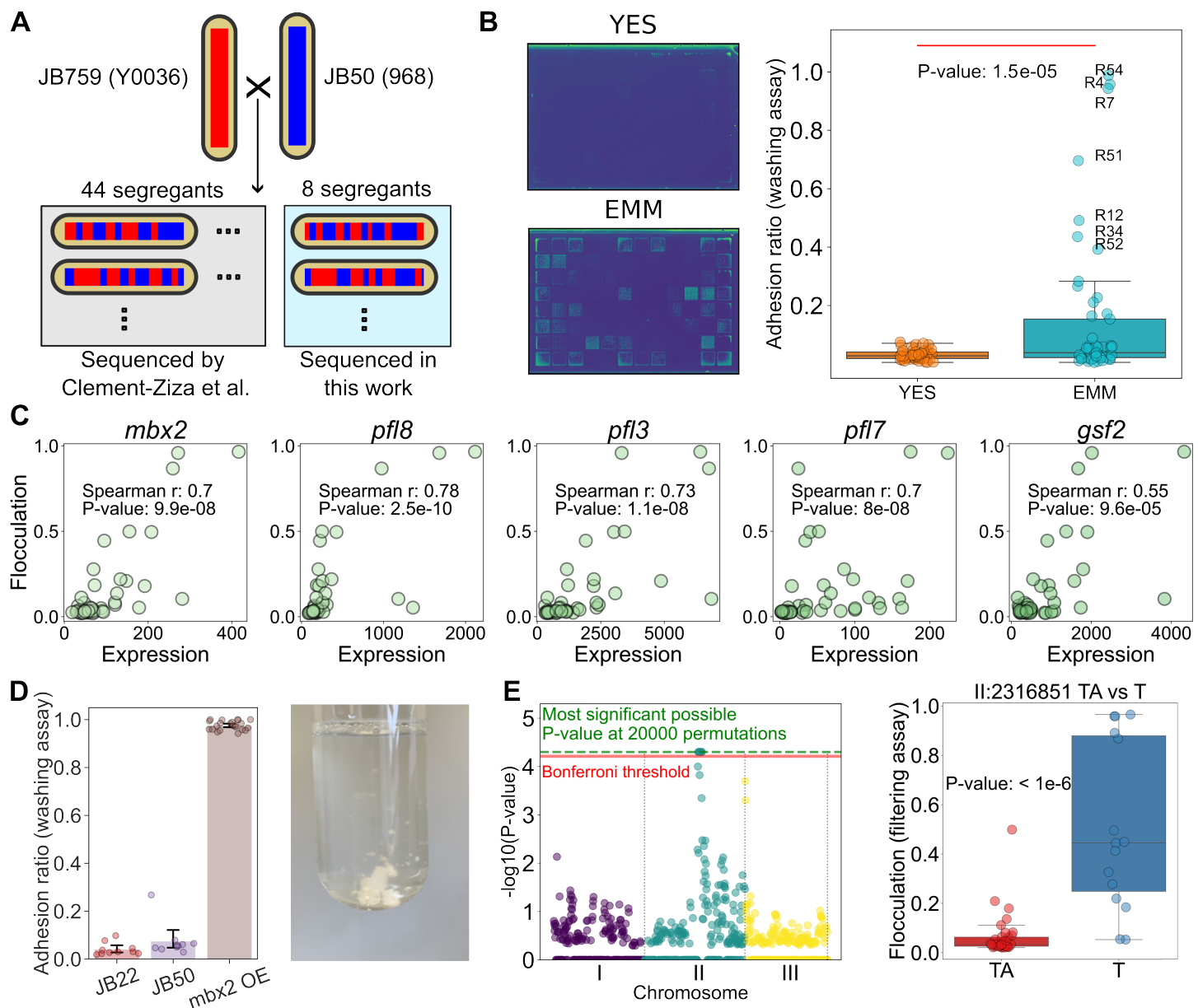


Figure 3: In the JB50-JB759 segregant library, MLP formation on EMM is driven by *mbx2* expression and is associated with a single-nucleotide deletion on chromosome II. A: Scheme for the segregant library. Red and blue stripes indicate recombination of the genome resulting from meiosis. SNPs for the strains inside the grey box were previously identified (46) and genome sequencing data for the strains in the light blue box were generated in this work (Methods). B: (Left) Example plates of segregant strains grown on EMM or YES are shown after washing shown in viridis colormap. (Right) Adhesion to agar of segregant strains on EMM (mean of 10 replicates) compared to YES (mean of 2 replicates). C: Correlation of *mbx2* and flocculin genes with flocculation in EMM. Each dot represents a strain from the segregant library. D: Barplot with measurements overlaid comparing adhesion measurements from standard laboratory *S. pombe* strains JB22 and JB50, and the *mbx2* overexpression strain generated in this work (Methods). E: (Left) Manhattan plot of our QTL analysis results for flocculation in EMM. Red line shows the Bonferroni-threshold, while the green dotted line shows the highest possible significance achievable using 20,000 permutations. (Middle, Right) Candidate variant is associated with both increased adhesion to agar (mean of 10 replicates) and increased flocculation in EMM (filtering assay, mean of 3 replicates). P-value determined using a permutation-based T-test with 1E+6 permutations.

Figure 4

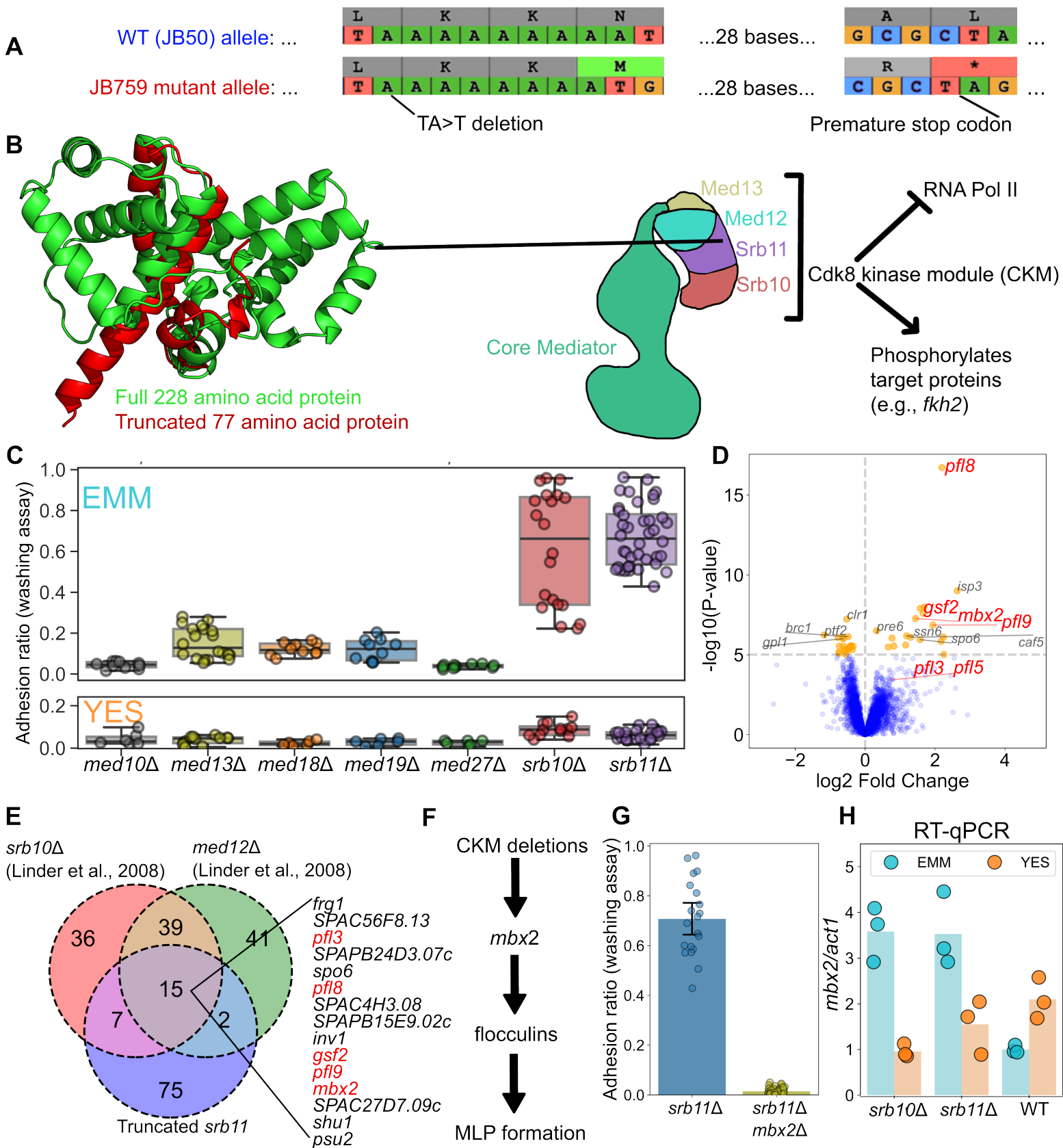


Figure 4: Cdk8 kinase module deletions upregulate *mbx2* in EMM, but not in YES, and lead to MLP formation. A: Scheme showing how a single nucleotide deletion leads to frameshift and premature stop-codon in *srb11*. B: Full *Srb11* structure (green) compared with the truncated *Srb11* structure (red) as predicted using Colabfold (121). Scheme on the right shows *Srb11* in the context of the Cdk8 kinase module of the Mediator complex. The structure was sketched based on structural data (78). C: Empirical cumulative distribution functions (ECDF) of adhesion values from Mediator gene deletion strains on EMM and YES. Each dot represents a replicate. Shaded regions show the 95% confidence intervals which were determined using 10,000 bootstrap samples. Percentiles where these confidence intervals do not overlap can be considered significantly different between any two strains. D: Differential expression analysis of segregant strains split on the II:2316851 TA>A single-nucleotide deletion. Fold-change values and P-values were obtained from DESeq2 (1). E: Overlap of upregulated genes in CKM

mutants based on our data and data from Linder et al. (1). F: Simplified model for how CKM deletions lead to MLP formation. G: Adhesion measurements for the *srB11* deletion strain obtained from the deletion collection, and its derived strain after *mbx2* knock-out with CRISPR. Each dot represents a replicate. H: RT-qPCR showing *mbx2* expression of *srB10Δ::Kan*, *srB11Δ::Kan* and WT strains in EMM or YES. Height of each bar reflects the mean of three biological replicates.

Figure 5

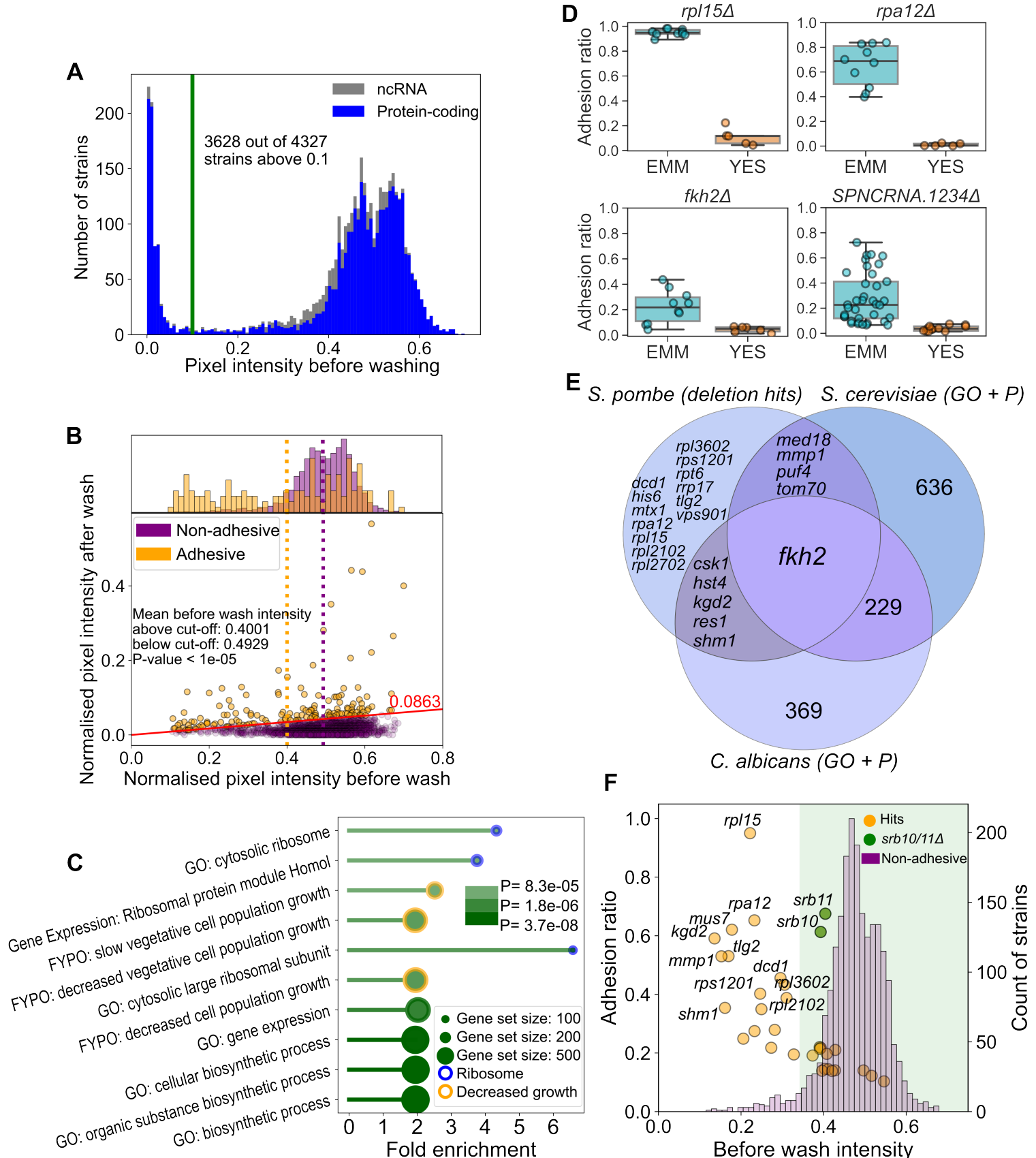


Figure 5: Our deletion library screen identified 31 genes associated with MLP formation on EMM. A: Histogram showing cell densities of strains in our deletion library screen before washing. B: Barplot showing the fold enrichment of the top-10 most significantly enriched processes, with blue outline for terms associated with ribosomes and orange outline for terms associated with decreased growth. Terms were sorted based on P-values and increasing color intensity represents increasing -log10(P-value). Additionally, the size of the circle at the end of each bar represents the size of the gene set. C: Scatterplot of mean cell densities before and after washing. Each dot represents a deletion strain, and colors represent adhesive and non-adhesive strains. The red line represents the cut-off at the 95th percentile of adhesion values, also shown on Supp Fig 9. The histogram shows the distribution of cell densities before washing as a proxy for growth. The dashed orange and purple lines mark the mean pre-wash intensity value for the two populations. P-value determined using a permutation-based T-test with

1E+5 permutations. D: Empirical cumulative distribution function (ECDF) of adhesion ratios for 4 of the 31 verified hits on EMM (light blue) vs YES (orange). Shaded regions show the 95% confidence intervals which were determined using 10,000 bootstrap samples. Percentiles where these confidence intervals do not overlap can be considered significantly different between the two conditions. E: Venn diagram showing the functional conservation of the genetically conserved hits from our screen. Only fkh2 is annotated as being involved in MLP formation in all three species. Venn diagram was made using matplotlib-venn in Python (120). F: Scatterplot of adhesion ratios and before-wash colony intensities overlaid by a histogram showing before-wash colony intensities of non-adhesive deletion strains which were assayed in the middle 60 spots during the original screen. The green shaded area marks strains that are above the 5th percentile of colony intensities in the non-adhesive strains. The *srb10/11 Δ* strains are highlighted with green, because they are the most adhesive strains from those with growth values above the 5th percentile.

Figure 6

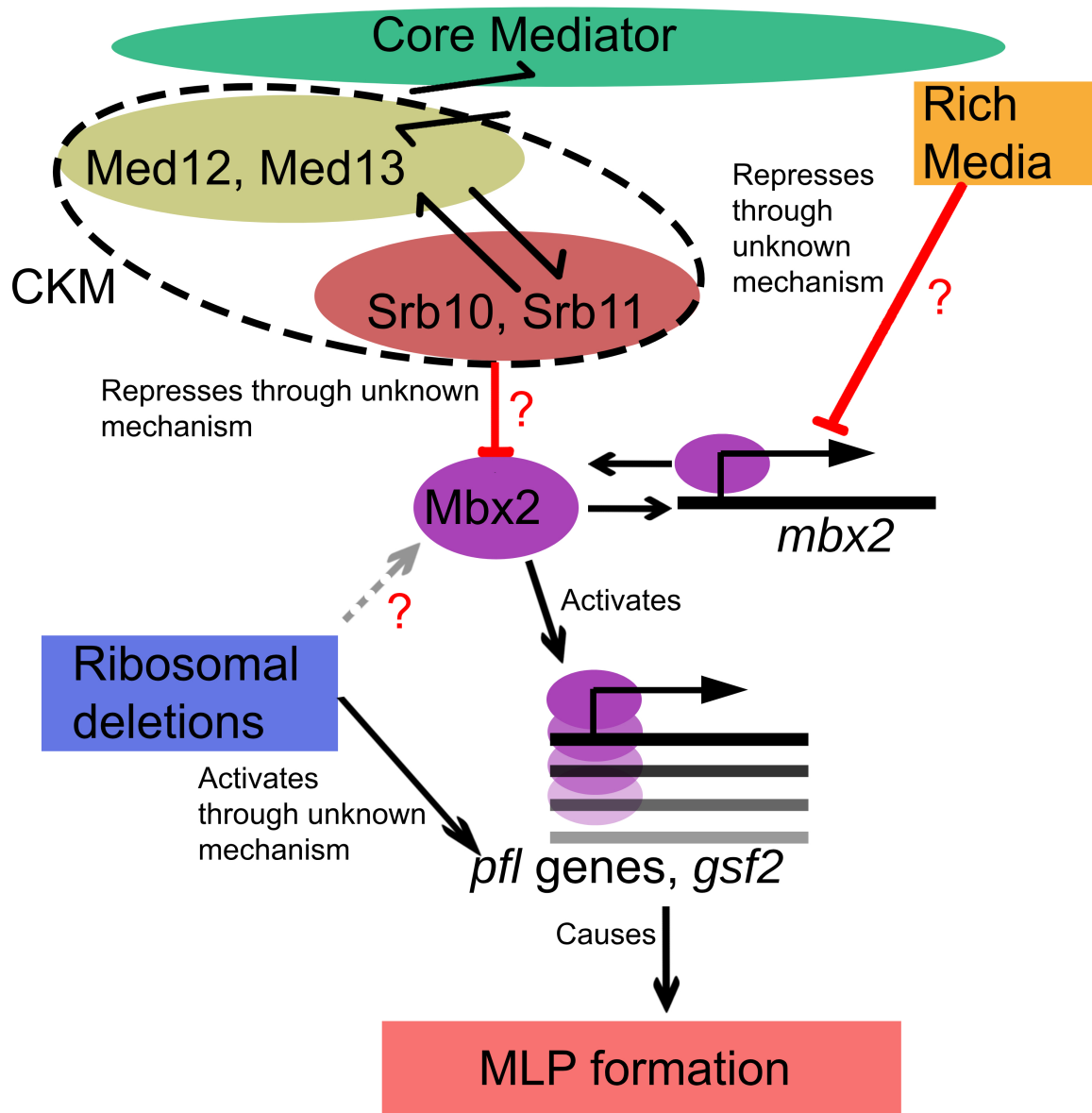
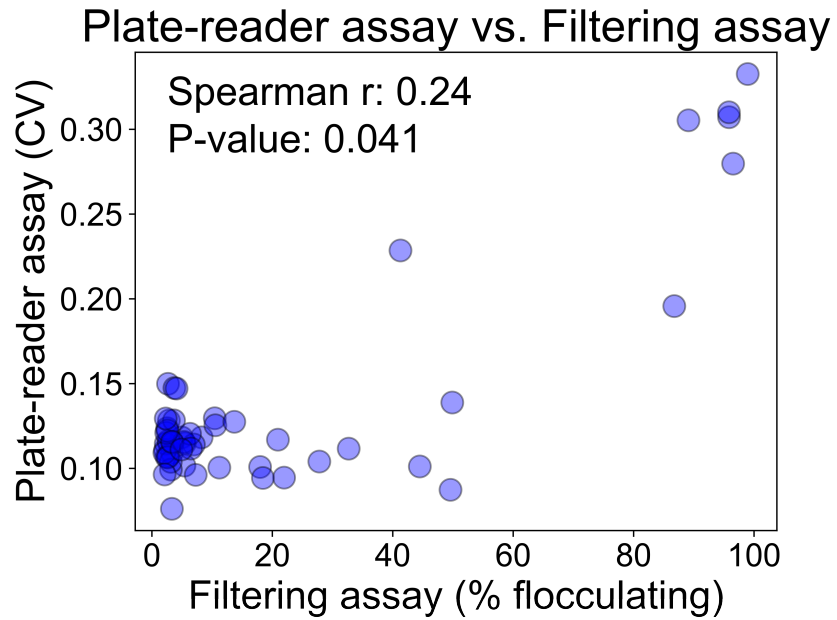
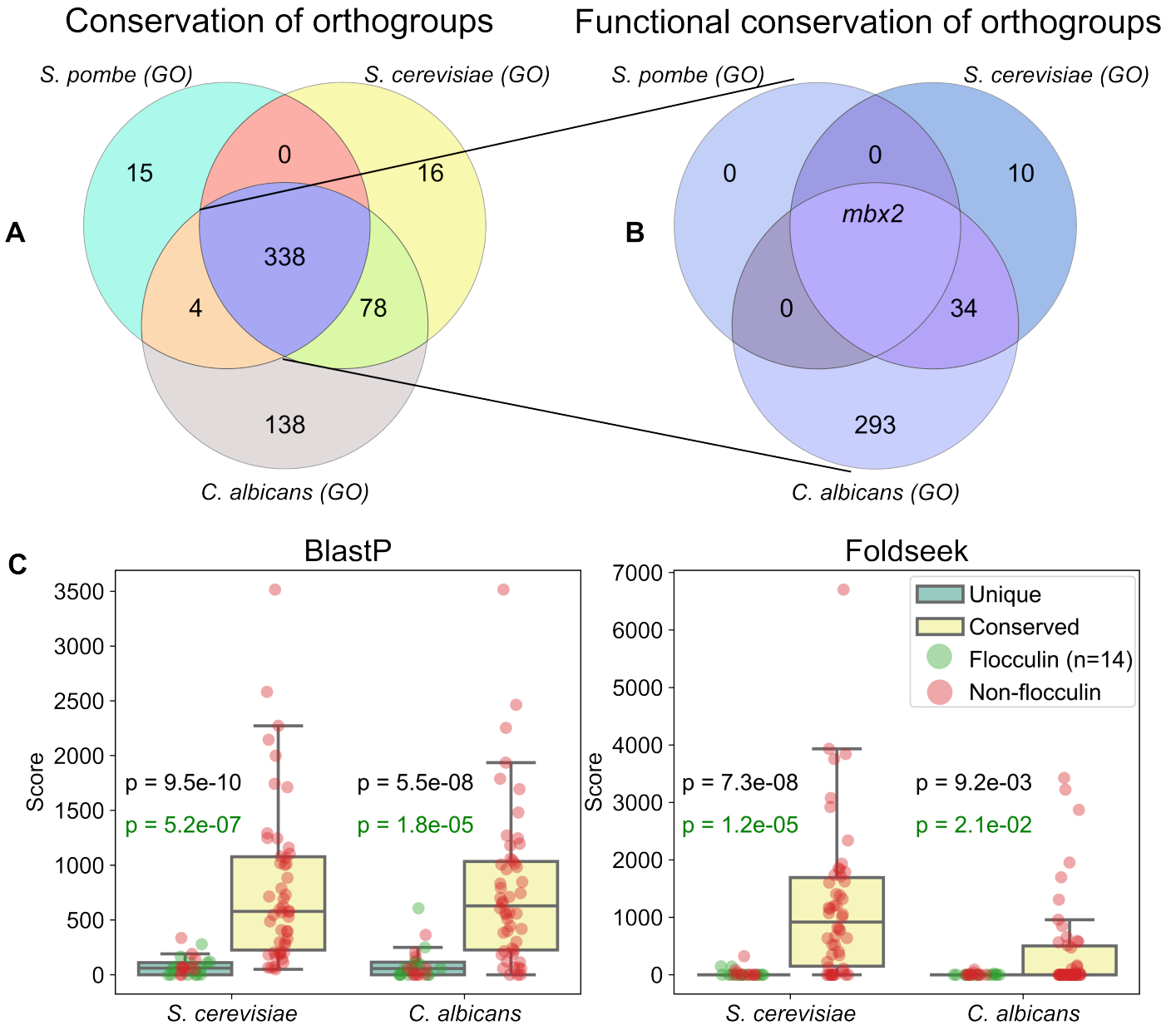


Figure 6: Model explaining EMM-dependent MLP formation of CKM mutants. Here we hypothesize that the CKM phosphorylates Mbx2 and targets it for degradation. Additionally, the *mbx2* transcript is repressed through an unknown mechanism in YES. In minimal media, when members of the CKM are deleted, *mbx2* becomes upregulated, triggering the expression of flocculin genes, which cause MLP formation. Additionally, deletion of ribosomal genes also triggers MLP formation, although it is unclear whether this occurs through upregulation of *mbx2* or directly through the flocculin genes. The coloured boxes show our main pathway of interest. The red arrows show our main contributions to the field, while red question marks show the main outstanding mechanistic questions.

Supplementary Figure 1

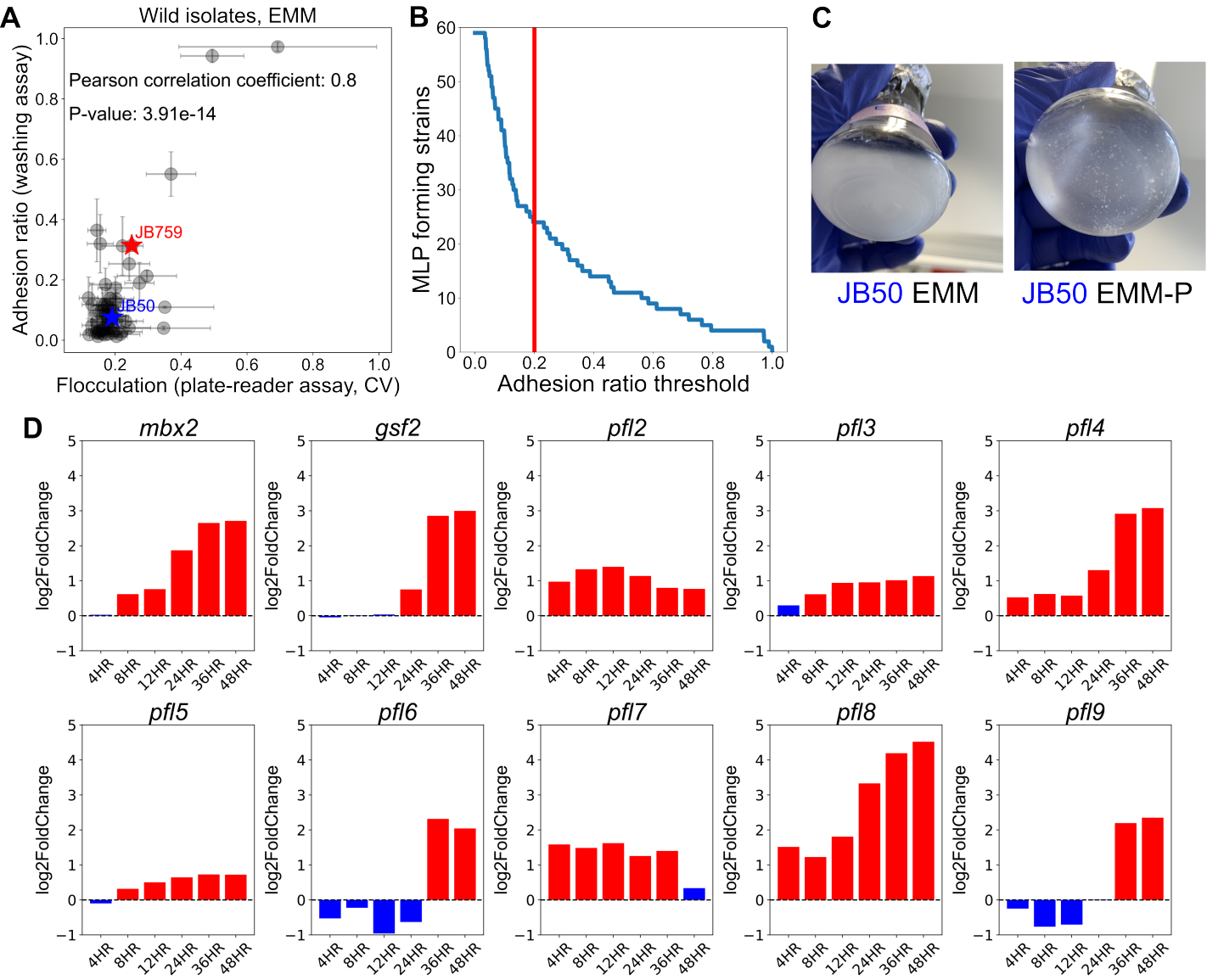


Supplementary Figure 2



Supplementary Figure 2: Conservation of MLP-related orthogroups between *S. pombe*, *S. cerevisiae* and *C. albicans*. A: Venn diagram representing genetic and functional conservation of orthogroups between the three species using data only from GO-terms. B: Comparison of “unique” and “conserved” genes using BLAST-P and Foldseek, see Methods. Each dot represents a given gene/protein. P-values were derived from Mann-Whitney U tests. Orange P-values were derived using the values of flocculin genes/proteins only, rather than all “unique” MLP-related genes/proteins.

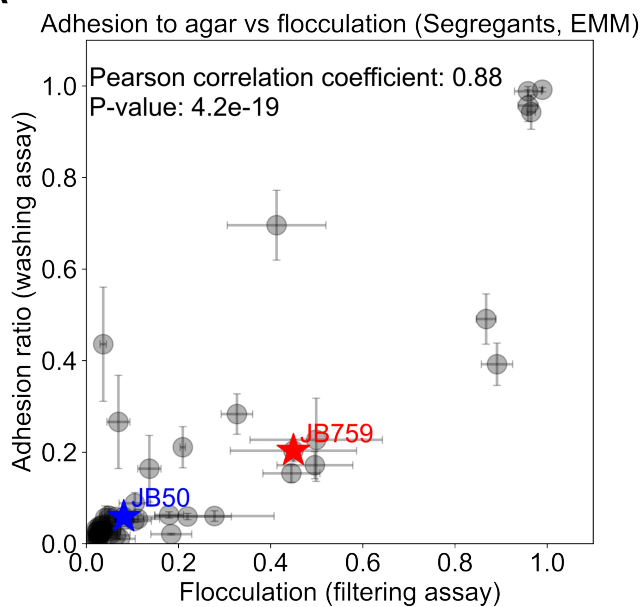
Supplementary Figure 3



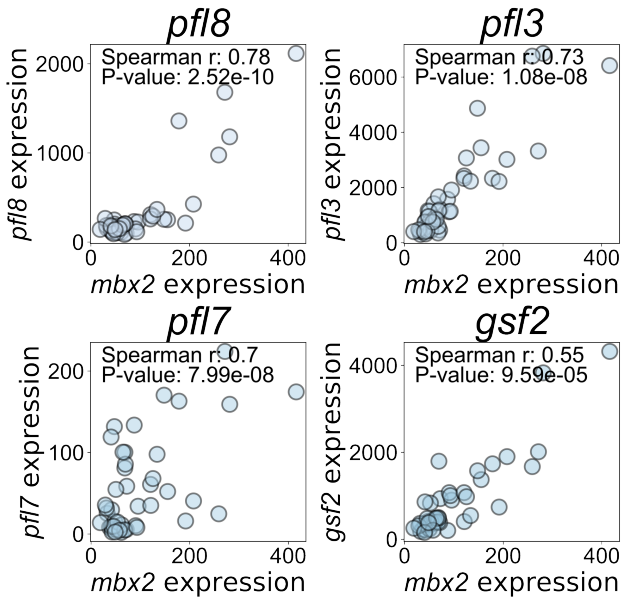
Supplementary Figure 3: Further analysis on adhesion phenotypes of the natural isolates across different conditions. A: Scatterplot comparison of flocculation and adhesion for the natural isolate library by measuring each strain with a high-throughput plate-reader assay (x-axis) and our high-throughput adhesion assay (y-axis). Each point represents the mean values for a strain with the standard error of the mean as error bars. B: Elbow plot of the number of strains designated as “MLP-forming” in at least one condition (y-axis) given different cut-off thresholds (x-axis). Empirically we found that 0.2 sits in the elbow of the plot, suggesting that it is a reasonable cut-off. C: Phosphate starvation induces MLP formation in the lab strain JB50. Images of the JB50 strain growing in 25ml flasks with 10ml media of either EMM (left) or EMM-P (right). Strains were first grown up on YES plates and then transferred to liquid cultures. There are clearly visible flocs forming in EMM-P. E: Barplot of log2FC in *mbx2* and flocculin expression at different timepoints during 2 days of phosphate starvation. Red bars represent significant log2FC values. Data taken from (75).

Supplementary Figure 4

A



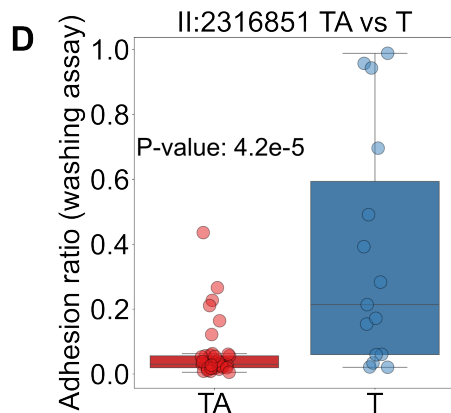
B



C



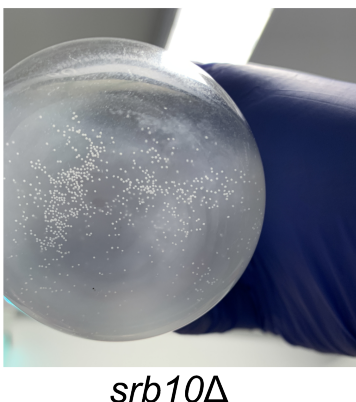
D



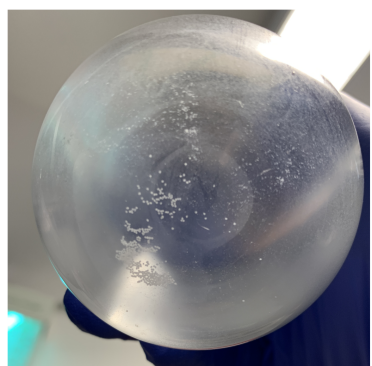
Supplementary Figure 4: Further analysis of the JB50-JB759 segregants and the role of *mbx2*. A: Scatterplot comparison of flocculation and adhesion for the JB50-JB759 library by measuring each strain with a filtering assay (x-axis) and our high-throughput adhesion assay (y-axis). Each point represents the mean values for a strain with the standard error of the mean as error bars. There is a strong correlation between the two MLPs. B: Scatterplot of expression levels of four flocculin genes against *mbx2* expression in the JB50-JB759 library (data from (46)), demonstrating a strong association. C: Results from the *mbx2* overexpression strain on EMM. (Left, Middle) Images of flocculating *mbx2*OE strain in EMM. (Right) Images of *mbx2*OE strain after thiamine addition resulting in no flocculation.

Supplementary Figure 5

A



srb10Δ



srb11Δ

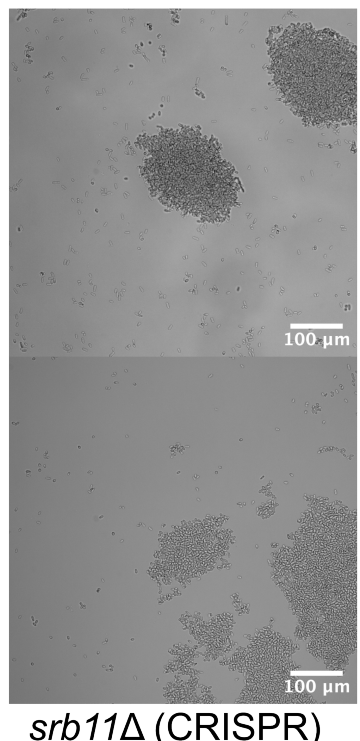
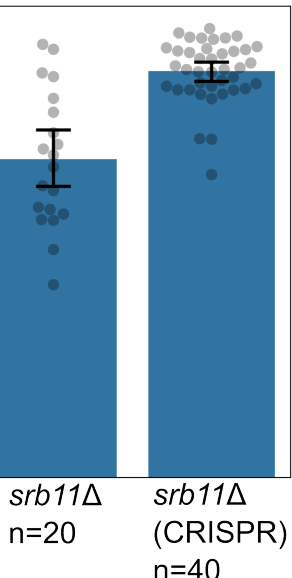
srb11Δ



C

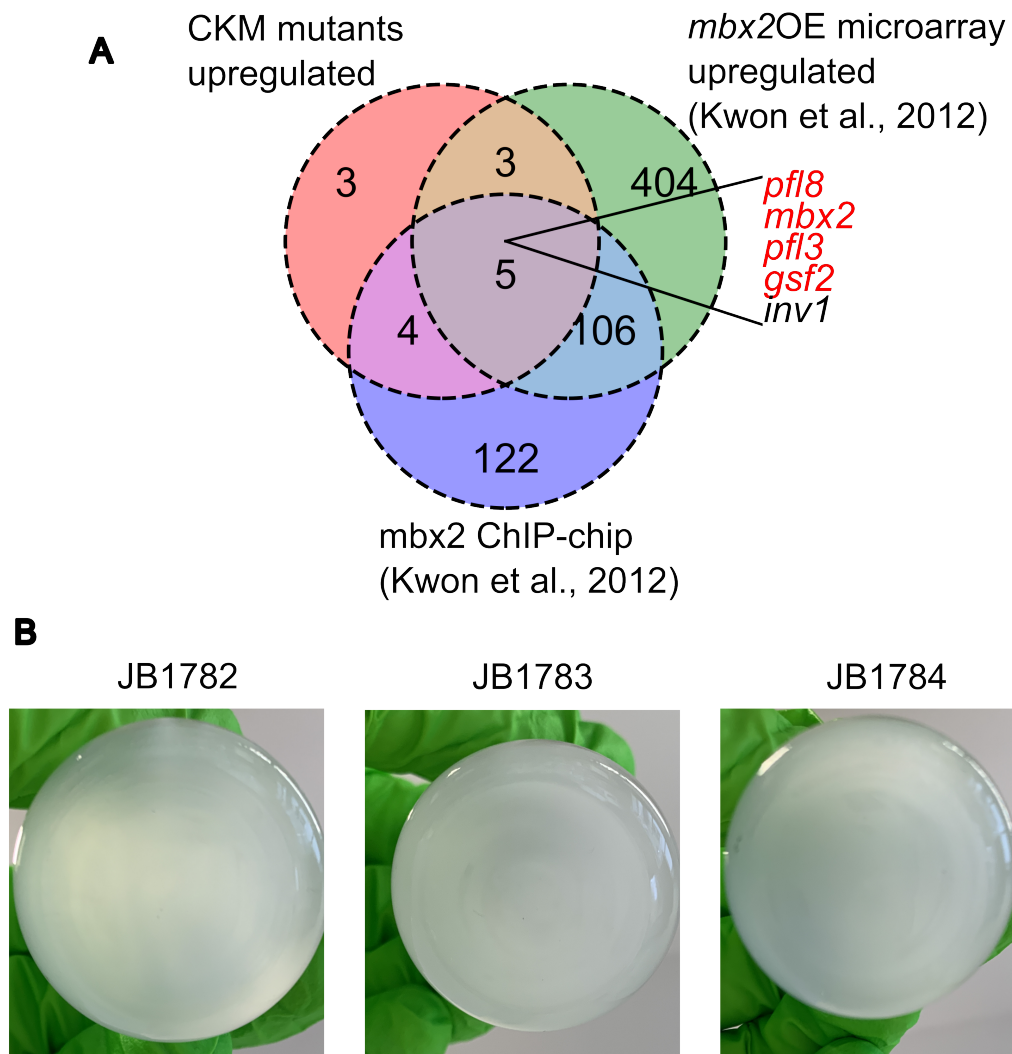
Adhesion ratio (washing assay)

P<1e-07



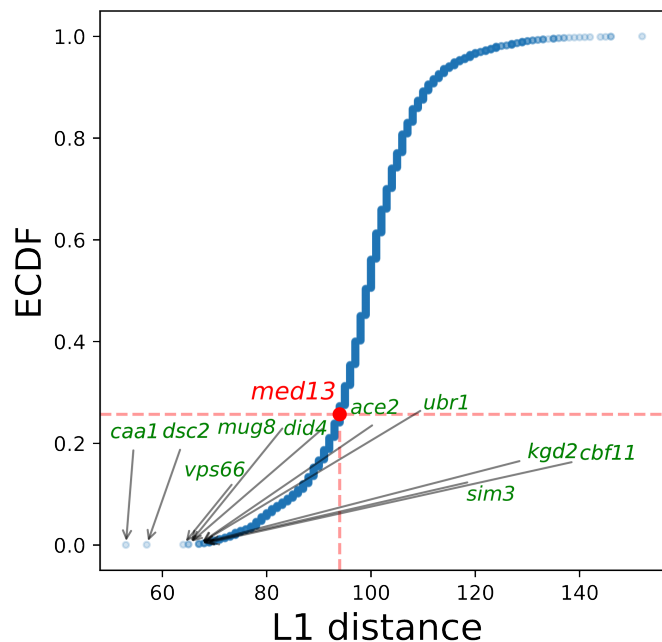
Supplementary Figure 5: The *srb10Δ* and *srb11Δ* strains show MLP formation. A: Images showing flocculating cultures of *srb10* and *srb11* in 250ml flasks grown in EMM. B: Validation of *srb11Δ::Kan* and CRISPR deletion strains used in the paper. Results from gel electrophoresis after PCR. Red rectangles mark the expected bands validating the strains. C: (Left) Barplot of adhesion values showing that the CRISPR deletion of *srb11* phenocopies the Kan deletion of *srb11* found in the deletion library. Additionally, we note that the CRISPR strain exhibits significantly stronger adhesion, likely because the deletion library strain has accumulated suppression mutations in other genes. Each dot is an independent measurement. (Right) Representative microscopy images of *srb11Δ::Kan* (top) and *srb11Δ (CRISPR)* (bottom) strains.

Supplementary Figure 6



Supplementary Figure 6: Mbx2 drives MLP formation in the *srb10 Δ* strain. A: Venn diagram showing the intersection of three gene sets: (i) Genes upregulated in CKM mutants, meaning upregulated in the *med12* and *srb10* microarray data from (61) and in the *srb11* truncated segregant RNA-seq data from (46), (ii) Genes upregulated after *mbx2* overexpression obtained from (25) and (iii) Genes bound by Mbx2 obtained from (25). B: Images showing non-flocculating cultures of three biological repeats (JB1782, JB1783, JB1784) of *srb11/mbx2* double delete strains.

Supplementary Figure 7

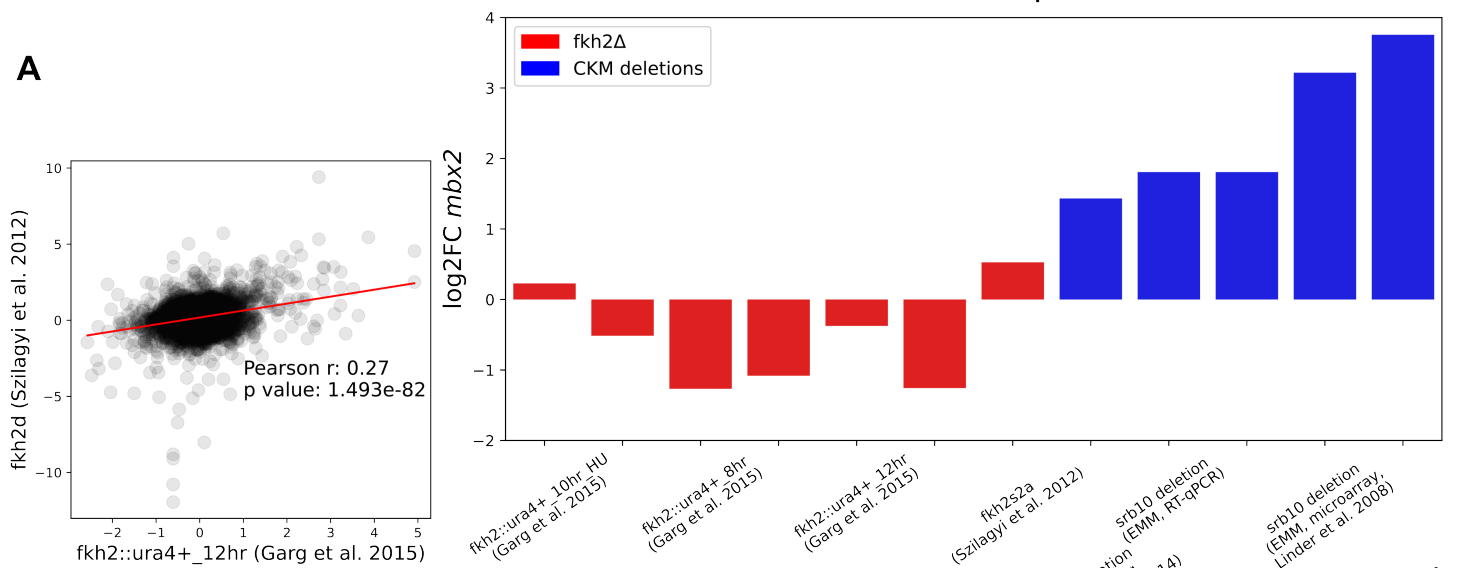


Supplementary Figure 7: In terms of the sensitivity/resistance phenotypes measured in (89), *srbl1* is not any more similar to *med13* than to an average deletion strain. Empirical cumulative distribution function of L1 distances (sum of differences across phenotypes; -1,0,1 are sensitive, neutral and resistant). Top 10 deletion strains closest in their phenotypes to *srbl1* are highlighted on the plot.

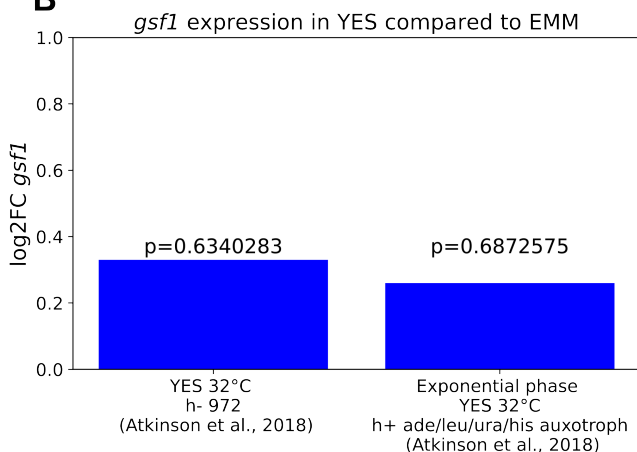
Supplementary Figure 8

mbx2 levels in *fkh2Δ* strains compared to CKM deletions

A

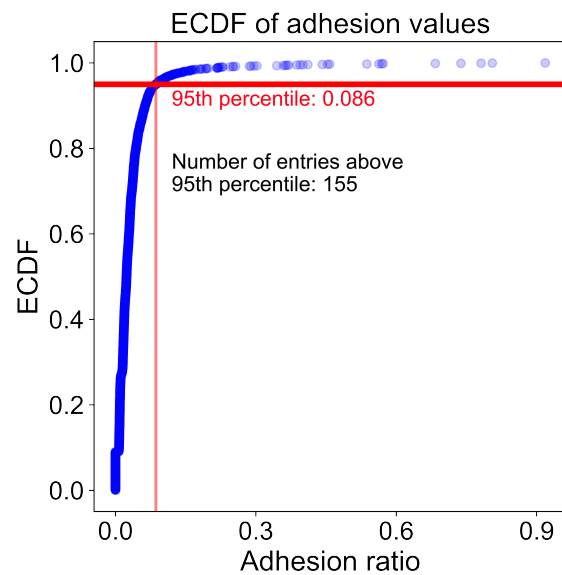


B



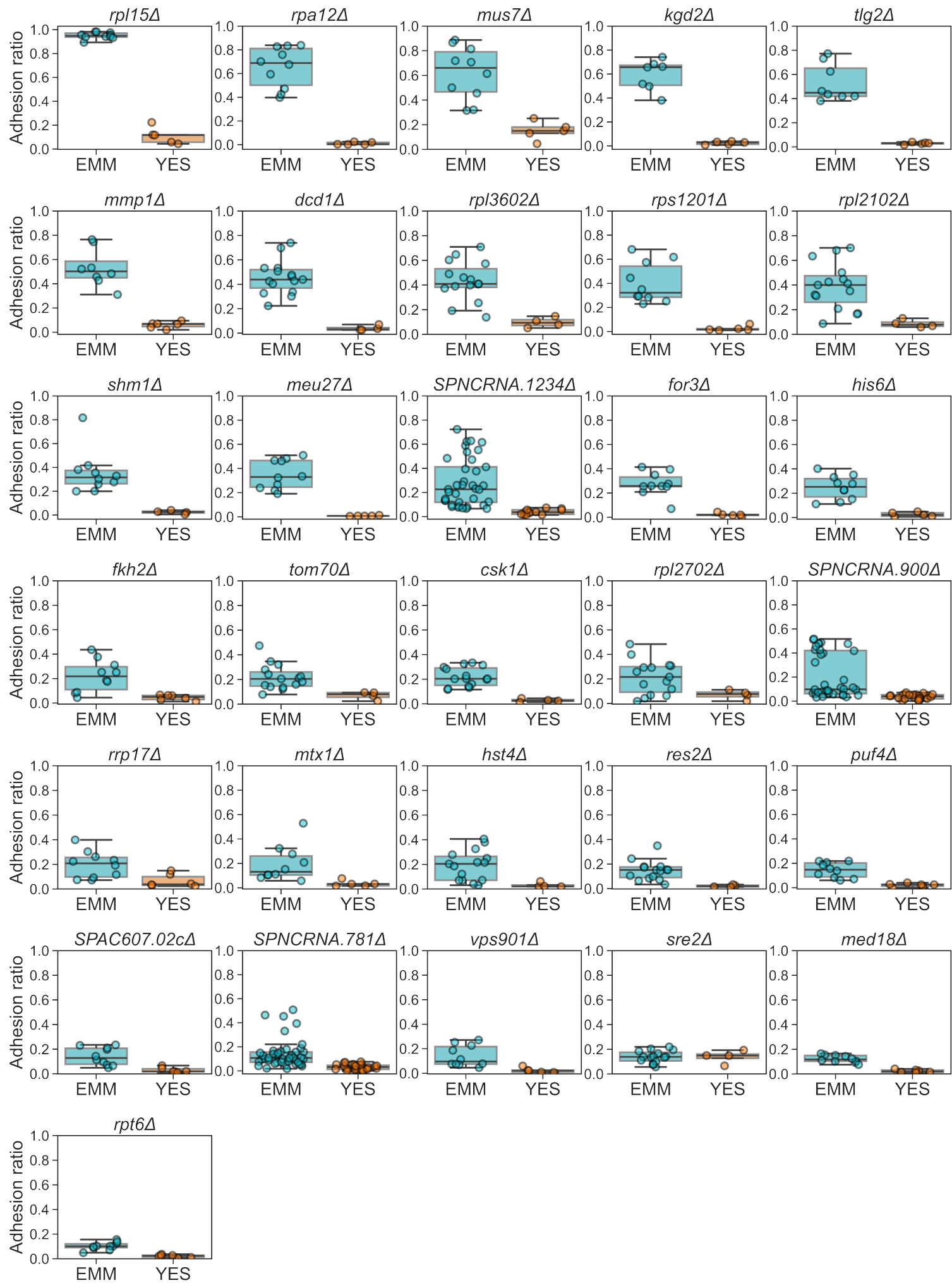
Supplementary Figure 8: Further analysis to deepen our understanding of the EMM-dependent upregulation of *mbx2* in CKM deletions. *Fkh2* is the only well-studied protein known to interact with the CKM in *S. pombe*, while *gsf1* is the only known transcription factor to repress *mbx2*. A: Scatterplot of fold changes comparing two different data sources for transcriptomic changes upon *fkh2* deletion. Each dot is a given gene in the dataset and the red line being a simple line of best fit. This plot concludes that it is fair to use the two data sources to draw joint conclusions from them. B: Barplot showing *log2 fold-changes* in *mbx2* expression levels upon *fkh2* deletion from (80) and (90) compared with expected fold changes from *med12* and *srb10* microarray data from (61) and in the *srp11* truncated segregant RNA-seq data from (46) and our RT-qPCR data collected in this work. C: Barplot showing *log2 fold-changes* in *gsf1* expression in YES compared to EMM. There is no significant upregulation in either of the two replicates. Data and P-values were taken from (1).

Supplementary Figure 9



Supplementary Figure 9: Empirical cumulative distribution function (ECDF) of adhesion ratios from the deletion library screen, with red lines showing the cut-off for the 95th percentile. Strains above the cut-off were used for enrichment analysis.

Supplementary Figure 10



Supplementary Figure 10: Empirical cumulative distribution function (ECDF) of adhesion ratios for the 31 verified hits on EMM (light blue) vs YES (orange). Shaded regions show the 95% confidence intervals which were determined using 10,000 bootstrap samples. Percentiles where these confidence intervals do not overlap can be considered significantly different between the two conditions. Note that there is only an overlap in the sre2 Δ strain.